Communication

# Using Binary Surfactant Mixtures to Simultaneously Improve Dimensional Tunability and Monodispersity in the Seeded-Growth of Gold Nanorods

Xingchen Ye, Chen Zheng, Jun Chen, Yuzhi Gao, and Christopher B. Murray

*Nano Lett.*, **Just Accepted Manuscript** • DOI: 10.1021/nl304478h • Publication Date (Web): 03 Jan 2013

# Using Binary Surfactant Mixtures to Simultaneously Improve Dimensional Tunability and Monodispersity in the Seeded-Growth of Gold Nanorods

*Xingchen Ye[1†], Chen Zheng[2†], Jun Chen[1], Yuzhi Gao[2], Christopher B. Murray[1, 2*]*

[1]Department of Chemistry and [2]Department of Materials Science and Engineering, University of Pennsylvania, Pennsylvania 19104, United States.

[†]These authors contributed equally to this work

# Abstract

We report a dramatically improved synthesis of colloidal gold nanorods (NRs) using a binary surfactant mixture composed of hexadecyltrimethylammonium bromide (CTAB) and sodium oleate (NaOL). Both thin (diameter < 25 nm) and thicker (diameter > 30 nm) gold NRs with exceptional monodispersity and broadly tunable longitudinal surface plasmon resonance can be synthesized using seeded growth at reduced CTAB concentrations (as low as 0.037 M). The CTAB-NaOL binary surfactant mixture overcomes the difficulty of growing uniform thick gold NRs often associated with the single-component CTAB system and greatly expands the dimensions of gold NRs that are accessible through a one-pot seeded growth process. Gold NRs with large overall dimensions and thus high scattering/absorption ratios are ideal for scattering-based applications such as biolabeling as well as enhancement of optical processes.


**Key Words:** gold nanorods, CTAB, sodium oleate, surfactant mixture, tetrahexahedral, plasmonics.

Gold nanorods (NRs) have received significant attention in recent years because of great promise for a wide array of applications including plasmon-enhanced spectroscopies,[1,2] bioimaging and therapeutics,[3-5] chemical sensing,[6,7] photonic and optoelectronic devices,[8] etc. The resonant excitation of the collective oscillations of free electrons confined to the NRs leads to the creation of localized surface plasmon resonances and large electric field enhancements near the NR surface.[9-11] One of the most intriguing properties of gold NRs is that their longitudinal surface plasmon resonance (LSPR), which can be excited by incident light polarized along the axial direction, depends strongly on the NR aspect ratio and therefore, can be synthetically tailored across a broad spectral range. Furthermore, the scattering and absorption cross sections at a given LSPR wavelength are largely determined by the overall size of gold NRs.[12] Therefore, the diameter of gold NRs can be an important differentiation factor for their applications. For example, extinction is dominated by absorption for thin gold NRs (diameter less than 15 nm), which makes them well-suited for photothermal applications that require high photon-to-heat conversion efficiency.[13] In contrast, scattering becomes dominant for thicker gold NRs (diameter larger than 30 nm), making them favorable for applications such as biolabeling[14] and enhancement of optical signals including metal-enhanced fluorescence[15] and surface-enhanced spectroscopies,[1,2] etc.

Since the seminal reports by Wang *et al.*,[16] Murphy *et al.*[17,18] and El-Sayed *et al.*,[19] seeded growth of colloidal gold NRs in the presence of cationic surfactant CTAB has been continuously optimized by many research groups.[2,20-30] A variety of additives such as acetone,[17] cyclohexane,[17] $Na_2S$,[27] hydrochloric acid or nitric acid,[26,31,32] iodide[33-35] and bromide ions[36-38], copper ions[39] and small aromatic molecules[40] have been introduced to the growth solution to affect gold NR growth. Importantly, El-Sayed *et al.* demonstrated that NRs grown in a binary surfactant mixture of

CTAB and benzyldimethylhexadecylammoniumchloride (BDAC) can achieve high aspect ratios ranging from 4.6 to 10 after aging of the growth solutions for 7-10 days, which the authors attributed to a more flexible nature of the binary surfactant templates compared to the single-component CTAB system as well as different affinities of the two surfactants on the facets of growing gold NRs.[19] Although nowadays, the original idea of using a high concentration of CTAB (0.1M, far beyond its first critical micelle concentration) as a soft template is not considered the primary role of CTAB during gold NR formation, these previous works suggest that it is possible to achieve greater tunability of NR's dimensions through judicious introduction of additional components to the NR growth solution. On the other hand, significant progress has been made on the size and shape tuning of gold NRs through multi-step processes such as direct overgrowth,[2,41,42] transverse overgrowth[12,43] and anisotropic oxidation[12,44] of preformed gold NRs. Despite these great progress, one-pot seeded growth of monodisperse thick gold NRs (diameter larger than 30 nm) with broadly tunable LSPR has remained quite challenging using existing synthetic procedures.

In this work, we report a dramatic improvement in the seeded growth of colloidal gold nanorods using binary surfactant mixtures. Monodisperse Au NRs with negligible shape impurities (less than 0.5 % of the total number of nanoparticles) can be obtained at much lower concentrations of CTAB (as low as 0.037 M) in the NR growth solution compared to the standard protocols (0.1 M). More importantly, the use of a secondary surfactant in addition to CTAB circumvents the limitations in NR's dimensional tunability (particularly NR's diameter) associated with prevailing synthetic procedures, allowing gold NRs having diameters between 15 and 50 nm and LSPR wavelength tunable from 650 nm to 1150 nm to be readily accessible in one-pot reactions.

A binary surfactant mixture composed of CTAB and sodium oleate (NaOL) is used in the gold NR growth solution. NaOL, the sodium salt of a long-chain unsaturated fatty acid, is an anionic surfactant soluble in water. The double bond in NaOL molecules allows them to slowly reduce $HAuCl_4$ in the absence of ascorbic acid (AA), as evidenced by the disappearance of orange-yellow color of dissolved gold salts (detailed synthetic procedures are described in Supporting Information). As a result, the optimal molar ratio between Au(III) and AA is found to be around 3:1 for the CTAB-NaOL system. In contrast, with commonly used methods, $HAuCl_4$-CTAB complexes are not reduced until AA is added to the growth solution, and therefore a molar ratio around 1.5 between AA and Au(III) is often employed.

Figure 1 and Figure S2 show TEM images of a collection of monodisperse gold NRs synthesized using 0.037 M CTAB and 0.0126 M NaOL in the growth solution. The aspect ratio of NRs can be continuously adjusted from 3.8 to 7.6 by varying the amounts of $AgNO_3$ and seed solutions as well as pH of growth solutions, as detailed in Table S2. Although concentrations of reagents and reaction parameters affect NR's dimensions in a complex and interrelated manner, the general trends are: 1) Lowering pH of growth solutions usually leads to a higher NR aspect ratio. A simultaneous increase in NR's length and decrease in NR's diameter can occur with more acidic growth solutions. Moreover, a greater percent change is often observed in NR's diameter at intermediate pH values, and in NR's length with very acidic growth solutions (pH around 1.0). The trend can be seen by comparing the dimensions of two sets of gold NRs shown Figure 1 and Figure S2: (1c, 1h, S2d and 1i) and (1b, 1f, S2c and 1g), both of which are NR samples synthesized with an increasing acidity of the growth solutions while other experimental conditions were kept unchanged. 2) Reducing the amount of seed particles often results in an increase in both length and diameter of gold NRs (Table S2). Figure 2 shows extinction spectra of

the NRs shown in Figure 1. The LSPR wavelength red-shifts from 790 nm to 1150 nm as aspect ratio of gold NRs increases. It is notable that a sharp ensemble LSPR is present in every NR sample (e.g. blue curve: fwhm= 110 nm or 0.185 eV for a LSPR at 857 nm; orange curve: fwhm= 130 nm or 0.173 eV for a LSPR at 967 nm; red curve: fwhm= 170 nm or 0.186 eV for a LSPR at 1068 nm), which further confirms the narrow size distribution of NRs. In addition, negligible amounts of shape impurities (e.g. spheres) are produced during NR formation as evidenced by the very weak absorption around 525 nm in the extinction spectra (Figure 2). Gold NRs with comparable size uniformity and shape purity especially those having LSPR wavelengths longer than 850 nm have rarely been demonstrated with either commonly used methods[19,31,45] or with the CTAB-aromatic additive systems.[40] We further study the growth of gold NRs using 0.047 M CTAB together with NaOL in the growth solution. As shown in Figures S4-S6, a rich array of uniform gold NRs with accessible dimensions comparable to those shown in Figure 1 and Figure S2 can be obtained. It is worth pointing out that gold NRs synthesized using 0.047M CTAB are consistently smaller in size (especially in diameter) than those made using 0.037 M CTAB provided other reaction conditions are identical (Table S2). This suggests that a high concentration of CTAB may promote NR formation through adsorbing onto the growing gold NRs and selectively blocking crystal growth along certain directions,[45] which may also be responsible for the limited range of NR dimensions achievable using well-established methods (0.1 M CTAB). Although seed-mediated growth of gold NRs having LSPR wavelength longer than 850 nm has been demonstrated using different strategies such as lowering the pH of growth solutions[31] or using CTAB/BDAC binary surfactants[19], the diameter of NRs is usually smaller than 20 nm and in most cases, less than 15 nm. On the other hand, as manifested in Figure 1 and Figures S2-S6, the CTAB-NaOL binary mixture may represent an intriguing alternative to the

single-component CTAB system since it allows monodisperse high aspect ratio gold NRs having diameter larger than 20 nm to be generated at comparable pH values of the growth solution.

To explore the possibility of growing thicker gold NRs (diameter > 30 nm), we further reduce the amount of seed particles added to the growth solution (Table S3). As shown in Figure 3 and Figure S7, monodisperse gold NRs having diameter between 30 and 45 nm and aspect ratios tunable from 2.2 to 5.0 can be achieved, corresponding to a spectral tunability of NR's LSPR wavelength from 660 nm to 970 nm (Figure 4). Within the pH range between 1.1 and 1.5 (Table S1), aspect ratio of gold NRs is largely determined by the acidity of growth solutions (Table S3). NRs of higher aspect ratios are generally attainable using more acidic growth media. The dimensions of gold NRs can be further adjusted by changing the amounts of $AgNO_3$ or seed particles. Furthermore, a lower concentration of CTAB tends to produce thicker NRs. For example, NRs shown in Figure 3c (made with 0.037M CTAB) are larger in diameter than those in Figure 3h (made with 0.047M CTAB), even though the latter are made with fewer seed particles present in the growth solution.

Using the CTAB-NaOL binary surfactant mixture, even thicker gold NRs (diameter > 45 nm) can be obtained as the seed volume is further reduced (Figures 5, 6, S8-S10 and Tables S4-S5). The combination of a minimum amount of seed particles and a fairly acidic growth solution (pH=1.10) yields gold NRs with an aspect ratio as high as 3.4 (Figure 5f), resulting in an LSPR centered at 895 nm (Figure 5h, blue curve). Figure 7 displays the extinction spectra of those thick gold NRs of similar aspect ratios as shown in Figure 6a-d. When the diameter of gold NRs is greater than a critical value, which is found to be about 50 nm, a further increase in NR's diameter leads to a gradual red-shift of the transverse plasmon band and a concomitant decrease in the ratio of intensities between the longitudinal and transverse plasmonic resonances (Figure 7). As

dimensions of gold NRs become larger, they start to develop clear faceting. Morphological studies using SEM show that thick gold NRs (diameter <100 nm) are elongated tetrahexahedral (ETHH) shaped, which is consistent with previous reports of ETHH gold nanocrystals (Figure 8a-c and Figure S11).[46-48] However, we do observe that in thicker gold NRs (diameter > 100 nm), additional truncations or facetings occur at the eight vertices where six facets meet on the ETHH NRs, giving rise to a total of 32 exposed facets as opposed to 24 as for an ETHH nanocrystal (Figure 8d-f).

To shed more light on gold NR formation in the CTAB-NaOL binary surfactant mixtures, a series of control experiments are conducted. Firstly, the cationic species of the oleate surfactant does not seem to influence the growth of gold NRs, as shown by the fact that NRs of similar dimensions and comparable quality can be synthesized by replacing NaOL with the same amount of potassium oleate as long as all other experimental parameters are kept identical (Figure S13). Secondly, replacing NaOL with other long-chain unsaturated surfactants such as sodium linoleate (having two double bonds) or oleylamine also leads to reduction of Au(III) to Au(I) before the addition of AA. In both cases, gold NRs can still be produced at high yields, albeit with slightly inferior size uniformity and shape purity (Figure S14). The reducing power of double bond in NaOL molecules towards Au(III) at room temperature is further confirmed by the absence of color disappearance when using sodium stearate, the saturated structural analog of NaOL. With sodium stearate, even though the same amount of AA as common methods (4.5 mL of 0.064 M AA solution at our scale) is added, yield of gold NRs is still very low and the amount of spheroidal impurities is significant (Figure S15). Thirdly, uniform gold NRs can only be produced with an acidic growth media using the CTAB-NaOL system (pH < 1.7). Since NaOL is a basic salt, adjusting the pH through addition of HCl is essential for gold NR formation (Figure S16a-c).

Fourthly, same level of control over NR's size uniformity as well as tunability in NR's dimensions is hardly achievable using the standard method (0.1M CTAB) given comparable acidities (pH < 1.5) of NR growth solutions (Figure S17). At a similar pH, yield of gold NRs drops dramatically when 0.047 M CTAB is used in the absence of NaOL (Figure S16d). Moreover, no gold NR formation occurs after 48 hours when the amount of AA is further reduced to [Au(III)]: [AA] = 4:1. Therefore, in the CTAB-NaOL binary surfactant system, a small amount of AA is still necessary to reduce Au(I) to $Au^0$ catalyzed by the seed particles. Furthermore, reducing Au(III) to Au(I) is not the sole role of NaOL. As shown in Table S6, a slight increase in the amount of NaOL (1 mmol) in the growth solution (without a measurable pH increase) consistently results in an increase in the diameter of gold NRs, provided all other growth conditions are kept the same. This suggests that NaOL molecules might mediate the binding between CTAB surfactants and certain facets of growing NRs.

In summary, we demonstrated that by using a binary surfactant mixture composed of CTAB and NaOL, gold NRs with simultaneously improved dimensional tunability and size uniformity compared to conventional methods can be synthesized while reducing the concentration of CTAB (as low as 0.037 M). Not only thin gold NRs (diameter smaller than 25 nm) with exceptional monodispersity and broadly tunable LSPRs can be made, but more importantly, thick gold NRs (diameter larger than 30 nm) with aspect ratios tunable up to 5.0 can be synthesized using seed-mediated growth. Although the LSPR wavelength of gold NRs is largely determined by their aspect ratios, the dimensions of NRs provide an effective means of tailoring the relative proportions of absorption and scattering that make up the extinction observed for the NRs at the LSPR frequency.[12] The CTAB-NaOL binary surfactant mixture overcomes the difficulty of growing monodisperse thick gold NRs associated with the single-component CTAB

system and greatly expands the dimensions of gold NRs that are accessible through a one-pot seeded growth process. Gold NRs with large overall dimensions and thus high scattering/absorption ratios are ideal for studies on plasmonic coupling[1,49] as well as scattering-based applications such as biolabeling[14] as well as enhancement of optical signals.[1,2,15]

## ASSOCIATED CONTENT

**Supporting Information**. Methods and detailed reaction conditions, additional TEM and SEM images, photographs of seed solution and nanorod growth solution, dark-field scattering image, results of control experiments. This material is available free of charge via the Internet at http://pubs.acs.org.

## AUTHOR INFORMATION

**Corresponding Author**

*Email: cbmurray@sas.upenn.edu.

## ACKNOWLEDGEMENT

X.Y., C.Z., Y.G., and C.B.M. acknowledge the support from the Office of Naval Research (ONR) Multidisciplinary University Research Initiative (MURI) on Optical Metamaterials through award N00014-10-1-0942. J.C. acknowledges the support from the MRSEC program of the National Science Foundation under award # DMR 11-20901. C.B.M. is also grateful to the Richard Perry University Professorship for support of his supervisor role.

REFERENCES

(1) Halas, N. J.; Lal, S.; Chang, W.-S.; Link, S.; Nordlander, P. *Chem. Rev.* **2011**, *111*, 3913-3961.
(2) Alvarez-Puebla, R. A.; Agarwal, A.; Manna, P.; Khanal, B. P.; Aldeanueva-Potel, P.; Carbo-Argibay, E.; Pazos-Perez, N.; Vigderman, L.; Zubarev, E. R.; Kotov, N. A.; Liz-Marzan, L. *Proc. Natl. Acad. Sci. USA* **2011**, *108*, 8157-8161.
(3) Wijaya, A.; Schaffer, S. B.; Pallares, I. G.; Hamad-Schifferli, K. *ACS Nano* **2009**, *3*, 80-86.
(4) Dreaden, E. C.; Alkilany, A. M.; Huang, X.; Murphy, C. J.; El-Sayed, M. A. *Chem. Soc. Rev.* **2012**, *41*, 2740-2779.
(5) Cobley, C. M.; Chen, J.; Cho, E. C.; Wang, L. V.; Xia, Y. *Chem. Soc. Rev.* **2011**, *40*, 44-56.
(6) Kabashin, A. V.; Evans, P.; Pastkovsky, S.; Hendren, W.; Wurtz, G. A.; Atkinson, R.; Pollard, R.; Podolskiy, V. A.; Zayats, A. V. *Nature Mater.* **2009**, *8*, 867-871.
(7) Liu, N.; Tang, M. L.; Hentschel, M.; Giessen, H.; Alivisatos, A. P. *Nature Mater.* **2011**, *10*, 631-636.
(8) Knight, M. W.; Sobhani, H.; Nordlander, P.; Halas, N. J. *Science* **2011**, *332*, 702-704.
(9) P Perez-Juste, J.; Pastoriza-Santos, I.; Liz-Marzan, L. M.; Mulvaney, P. *Coord. Chem. Rev.* **2005**, *249*, 1870-1901.
(10) Vigderman, L.; Khanal, B. P.; Zubarev, E. R. *Adv. Mater.* **2012**, *24*, 4811-4841.
(11) Chen, H.; Shao, L.; Li, Q.; Wang, J. *Chem. Soc. Rev.* **2013**, DOI: 10.1039/C2CS35367A.
(12) Ni, W.; Kou, X.; Yang, Z.; Wang, J. F. *ACS Nano* **2008**, *2*, 677-686.
(13) Huang, X.; Neretina, S.; El-Sayed, M. A. *Adv. Mater.* **2009**, *21*, 4880-4910.
(14) Rostro-Kohanloo, B. C.; Bickford, L. R.; Payne, C. M.; Day, E. S.; Anderson, L. J. E.; Zhong, M.; Lee, S.; Mayer, K. M.; Zal, T.; Adam, L.; Dinney, C. P. N.; Drezek, R. A.; West, J. L.; Hafner, J. H. *Nanotechnology* **2009**, *20*, 434005.
(15) Lakowicz, J. R.; Ray, K.; Chowdhury, M.; Szmacinski, H.; Fu, Y.; Zhang, J.; Nowaczyk, K. *Analyst* **2008**, *133*, 1308-1346.
(16) Yu, Y. Y.; Chang, S. S.; Lee, C. L.; Wang, C. R. C. *J. Phys. Chem. B* **1997**, *101*, 6661.
(17) Jana, N. R.; Gearheart, L.; Murphy, C. J. *Adv. Mater.* **2001**, *13*, 1389-1393.
(18) Jana, N. R.; Gearheart, L.; Murphy, C. J. *J. Phys. Chem. B* **2001**, *105*, 4065-4067.
(19) Nikoobakht, B.; El-Sayed, M. A. *Chem. Mater.* **2003**, *15*, 1957-1962.
(20) Busbee, B. D.; Obare, S. O.; Murphy, C. J. *Adv. Mater.* **2003**, *15*, 414-416.
(21) Gole, A.; Murphy, C. J. *Chem. Mater.* **2004**, *16*, 3633-3640.
(22) Sau, T. K.; Murphy, C. J. *Langmuir* **2004**, *20*, 6414-6420.
(23) Liu, M. Z.; Guyot-Sionnest, P. *J. Phys. Chem. B* **2005**, *109*, 22192-22200.
(24) Perez-Juste, J.; Liz-Marzan, L. M.; Carnie, S.; Chan, D. Y. C.; Mulvaney, P. *Adv. Func. Mater.* **2004**, *14*, 571-579.
(25) Taub, N.; Krichevski, O.; Markovich, G. *J. Phys. Chem. B* **2003**, *107*, 11579-11582.
(26) Wu, H. Y.; Chu, H. C.; Kuo, T. J.; Kuo, C. L.; Huang, M. H. *Chem. Mater.* **2005**, *17*, 6447-6451.
(27) Zweifel, D. A.; Wei, A. *Chem. Mater.* **2005**, *17*, 4256-4261.
(28) Jiang, X. C.; Brioude, A.; Pileni, M. P. *Colloids Surf. A* **2006**, *277*, 201-206.
(29) Kou, X. S.; Zhang, S. Z.; Tsung, C. K.; Yang, Z.; Yeung, M. H.; Stucky, G. D.; Sun, L. D.; Wang, J. F.; Yan, C. H. *Chem. Eur. J.* **2007**, *13*, 2929-2936.

(30) Guerrero-Martinez, A.; Perez-Juste, J.; Carbo-Argibay, E.; Tardajos, G.; Liz-Marzan, L. M. *Angew. Chem. Int. Ed.* **2009**, *48*, 9484-9488.
(31) Zhu, J.; Yong, K.-T.; Roy, I.; Hu, R.; Ding, H.; Zhao, L.; Swihart, M. T.; He, G. S.; Cui, Y.; Prasad, P. N. *Nanotechnology* **2010**, *21*, 285106.
(32) Kim, F.; Sohn, K.; Wu, J.; Huang, J. *J. Am. Chem. Soc.* **2008**, *130*, 14442-14443.
(33) Smith, D. K.; Miller, N. R.; Korgel, B. A. *Langmuir* **2009**, *25*, 9518-9524.
(34) Smith, D. K.; Korgel, B. A. *Langmuir* **2008**, *24*, 644-649.
(35) Rayavarapu, R. G.; Ungureanu, C.; Krystek, P.; van Leeuwen, T. G.; Manohar, S. *Langmuir* **2010**, *26*, 5050-5055.
(36) Sau, T. K.; Murphy, C. J. *Philos. Mag.* **2007**, *87*, 2143-2158.
(37) Garg, N.; Scholl, C.; Mohanty, A.; Jin, R. C. *Langmuir*, **2010**, *26*, 10271-10276.
(38) Si, S.; Leduc, C.; Delville, M.-H.; Lounis, B. *ChemPhysChem* **2012**, *13*, 193-202.
(39) Wen, T.; Hu, Z.; Liu, W.; Zhang, H.; Hou, S.; Hu, X.; Wu, X. *Langmuir* **2012**, DOI: 10.1021/la304181k.
(40) Ye, X.; Jin, L.; Caglayan, H.; Chen, J.; Xing, G.; Zheng, C.; Doan-Nguyen, V.; Kang, Y.; Engheta, N.; Kagan, C. R.; Murray, C. B. *ACS Nano* **2012**, *6*, 2804-2817.
(41) Song, J. H.; Kim, F.; Kim, D.; Yang, P. *Chem. Eur. J.* **2005**, *11*, 910-916.
(42) Sohn, K.; Kim, F.; Pradel, K. C.; Wu, J.; Peng, Y.; Zhou, F.; Huang, J. *ACS Nano* **2009**, *3*, 2191-2198.
(43) Kou, X. S.; Zhang, S. Z.; Yang, Z.; Tsung, C. K.; Stucky, G. D.; Sun, L. D.; Wang, J. F.; Yan, C. H. *J. Am. Chem. Soc.* **2007**, *129*, 6402-6404.
(44) Tsung, C. K.; Kou, X. S.; Shi, Q. H.; Zhang, J. P.; Yeung, M. H.; Wang, J. F.; Stucky, G. D. *J. Am. Chem. Soc.* **2006**, *128*, 5352-5353.
(45) Murphy, C. J.; Thompson, L. B.; Chernak, D. J.; Yang, J. A.; Sivapalan, S. T.; Boulos, S. P.; Huang, J. Y.; Alkilany, A. M.; Sisco, P. N. *Curr. Opin. Colloid Interface Sci.* **2011**, *16*, 128-134
(46) Ming, T.; Feng, W.; Tang, Q.; Wang, F.; Sun, L.; Wang, J.; Yan, C. *J. Am. Chem. Soc.* **2009**, *131*, 16350-16351.
(47) Yin, P.-G.; You, T.-T.; Tan, E.-Z.; Li, J.; Lang, X.-F.; Jiang, L.; Guo, L. *J. Phys. Chem. C* **2011**, *115*, 18061-18069.
(48) Kim, D. Y.; Im, S. H.; Park, O. O. *Cryst. Growth Des.* **2010**, *10*, 3321-3323.
(49) Funston, A. M.; Novo, C.; Davis, T. J.; Mulvaney, P. *Nano Lett.* **2009**, *9*, 1651-1658.

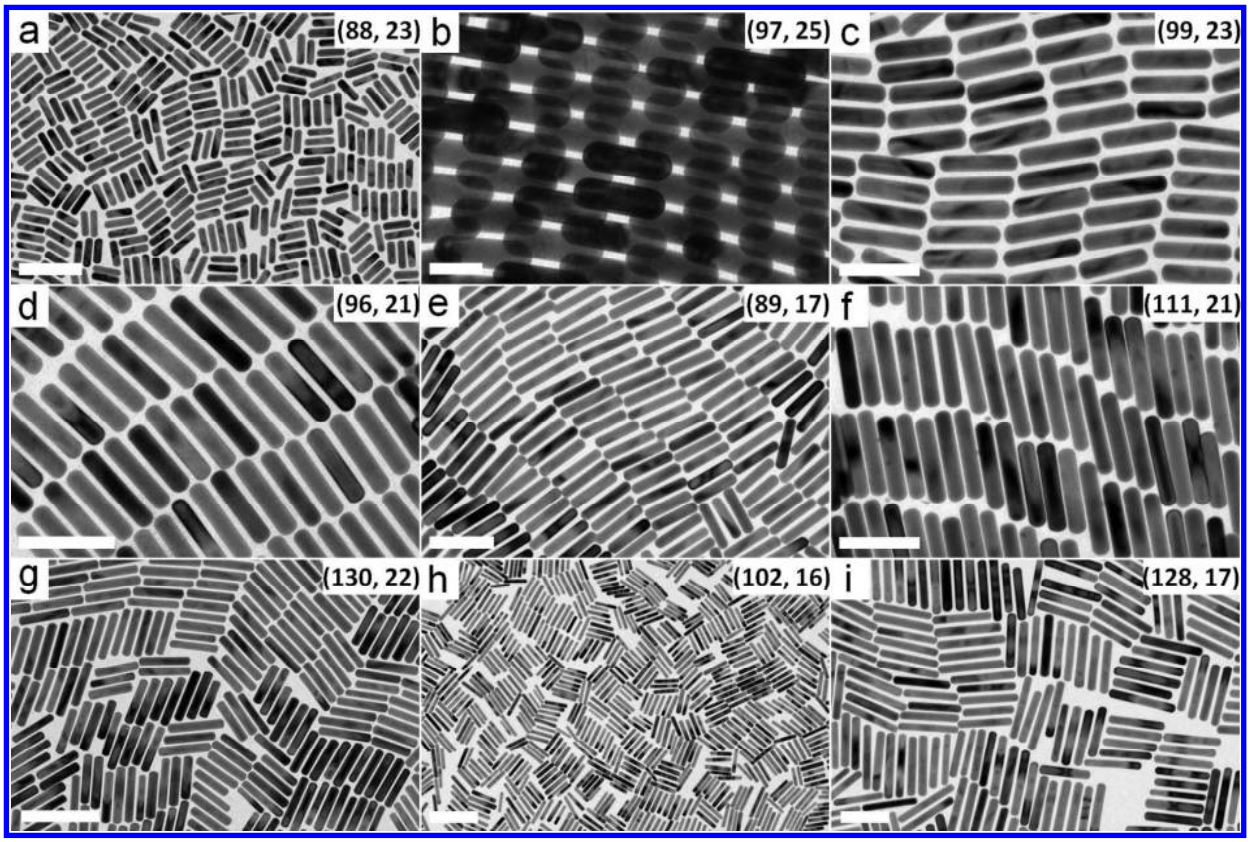


**Figure 1.** (a-i) TEM images of gold NRs having LSPR wavelengths longer than 700 nm and diameters less than 25 nm, arranged in the order of increasing aspect ratio from Figure 1a to Figure 1i. Insets are the average length and diameter (in nm) of the NRs determined by measuring the dimensions of at least 50 NRs from their TEM images. All NRs were synthesized using 0.037 M CTAB and 0.0078 M NaOL in the growth solution (assuming a total volume of 520 mL) and the growth conditions are detailed in Table S2. Scale bars: a) 200 nm, b) 50 nm, c-f) 100 nm, g-h) 200 nm, i) 100 nm.

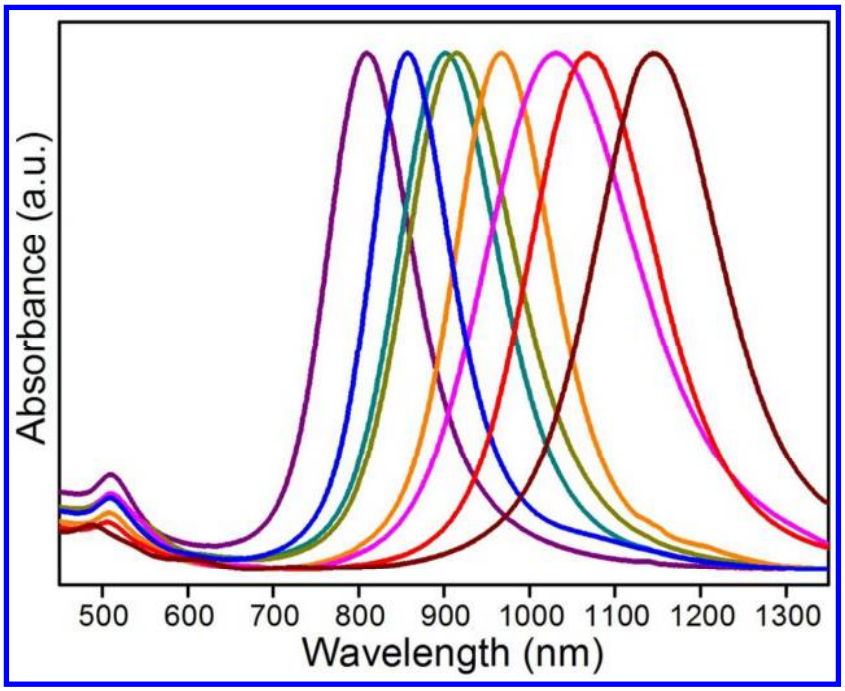


**Figure 2.** Normalized extinction spectra of gold NRs shown in Figure 1. As NR's aspect ratio increases from Figure 1a to Figure 1i, corresponding LSPR shifts towards longer wavelengths. Spectrum of the sample shown in Figure 1b is not included because it almost overlaps with that of the sample shown in Figure 1a (purple curve).

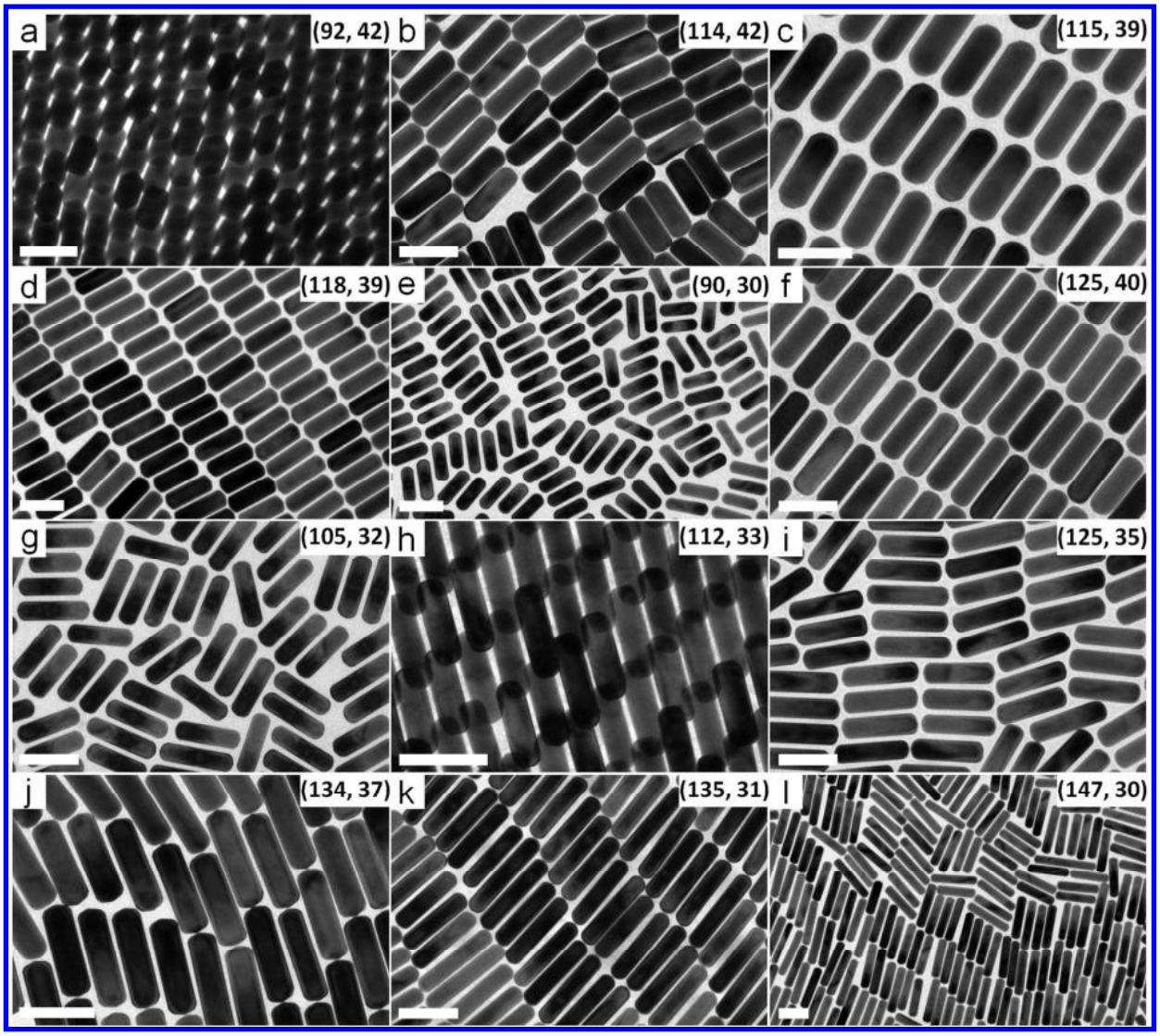


**Figure 3.** (a-l) TEM images of gold NRs having LSPR wavelengths longer than 650 nm and diameters between 25 and 45 nm, arranged in the order of increasing aspect ratio from Figure 1a to Figure 1l. Insets are the average length and diameter (in nm) of the NRs determined by measuring the dimensions of at least 50 NRs from their TEM images. The growth conditions are detailed in Table S3. All scale bars represent 100 nm.

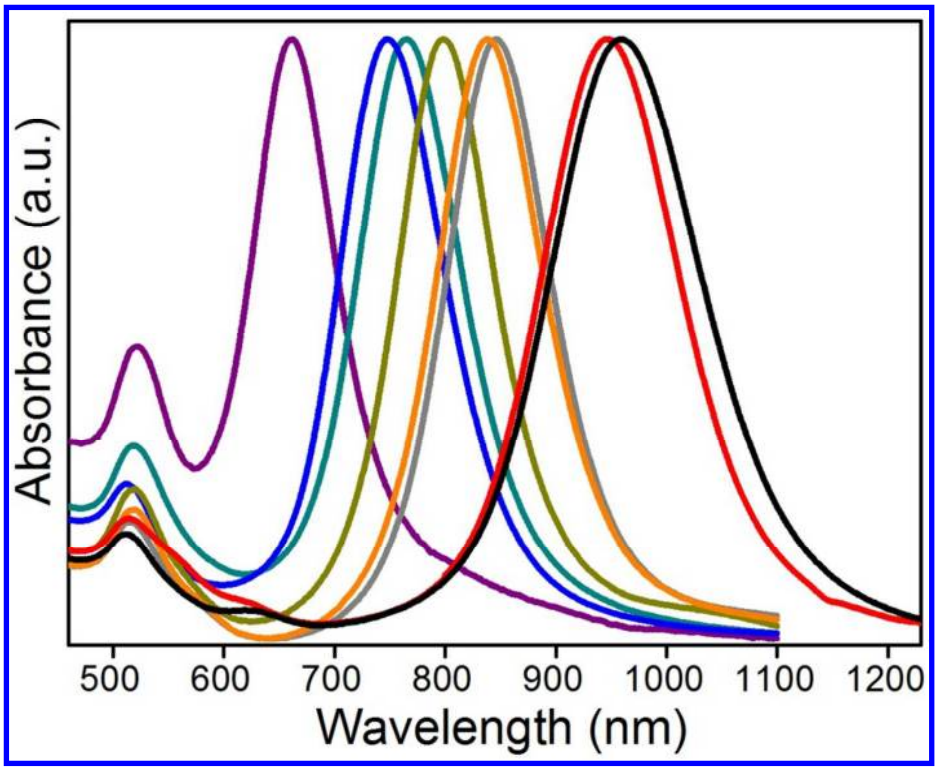


**Figure 4.** Normalized extinction spectra of gold NRs shown in Figures 3a (purple curve), 3c (blue curve), 3d (dark cyan curve), 3f (dark yellow curve), 3i (orange curve), 3j (gray curve), 3k (red curve) and 3l (black curve).

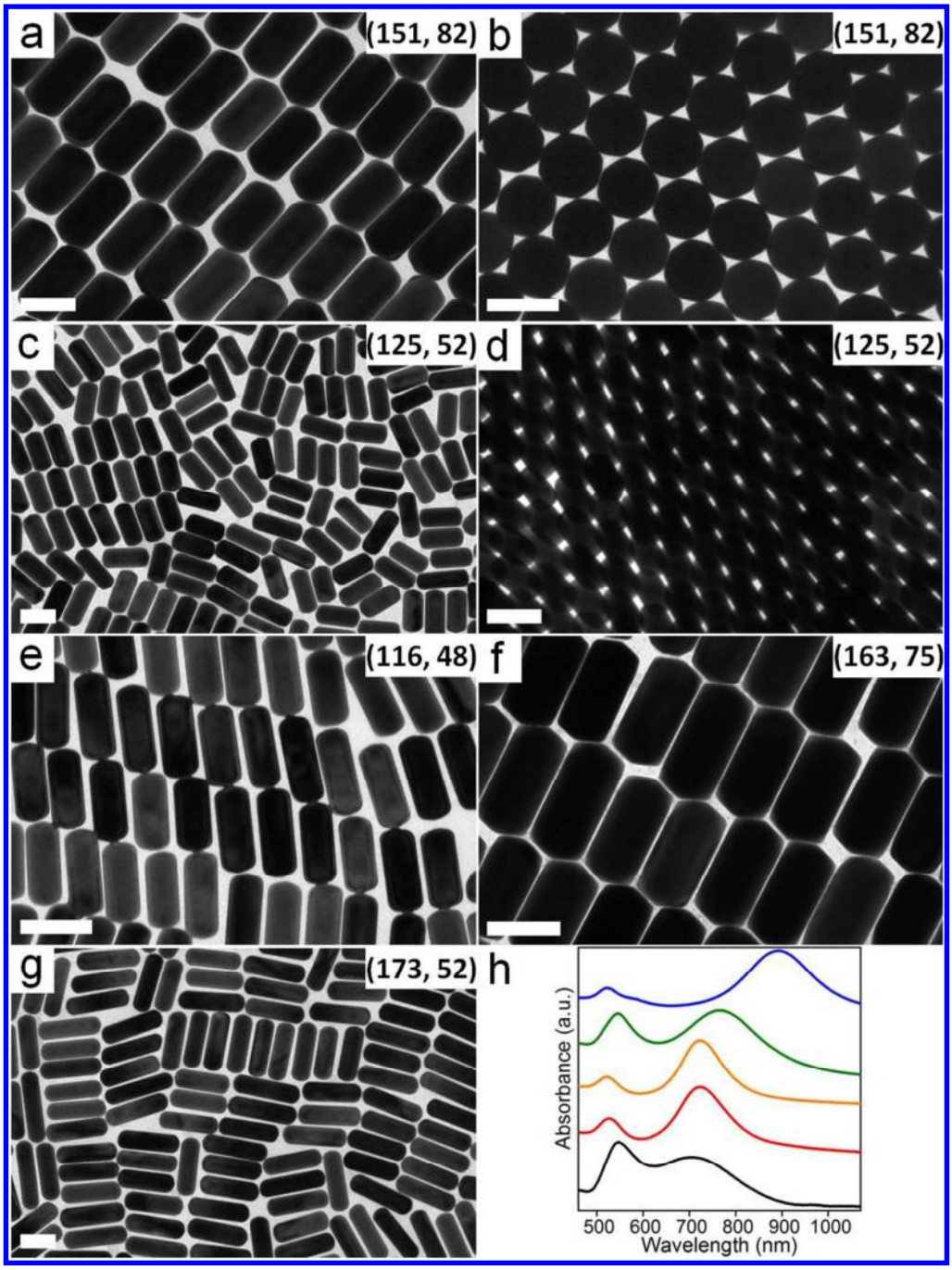


**Figure 5.** (a-g) TEM images of gold NRs having LSPR wavelengths longer than 700 nm and diameters greater than 45 nm. Insets are the average length and diameter (in nm) of the NRs determined by measuring the dimensions of at least 50 NRs from their TEM images. The growth conditions are detailed in Table S4. (h) Normalized extinction spectra of gold NRs shown in a-b (black curve), c-d (red curve), e (orange curve), f (green curve) and g (blue curve), respectively. All scale bars represent 100 nm. The spectra have been offset vertically for clarity.

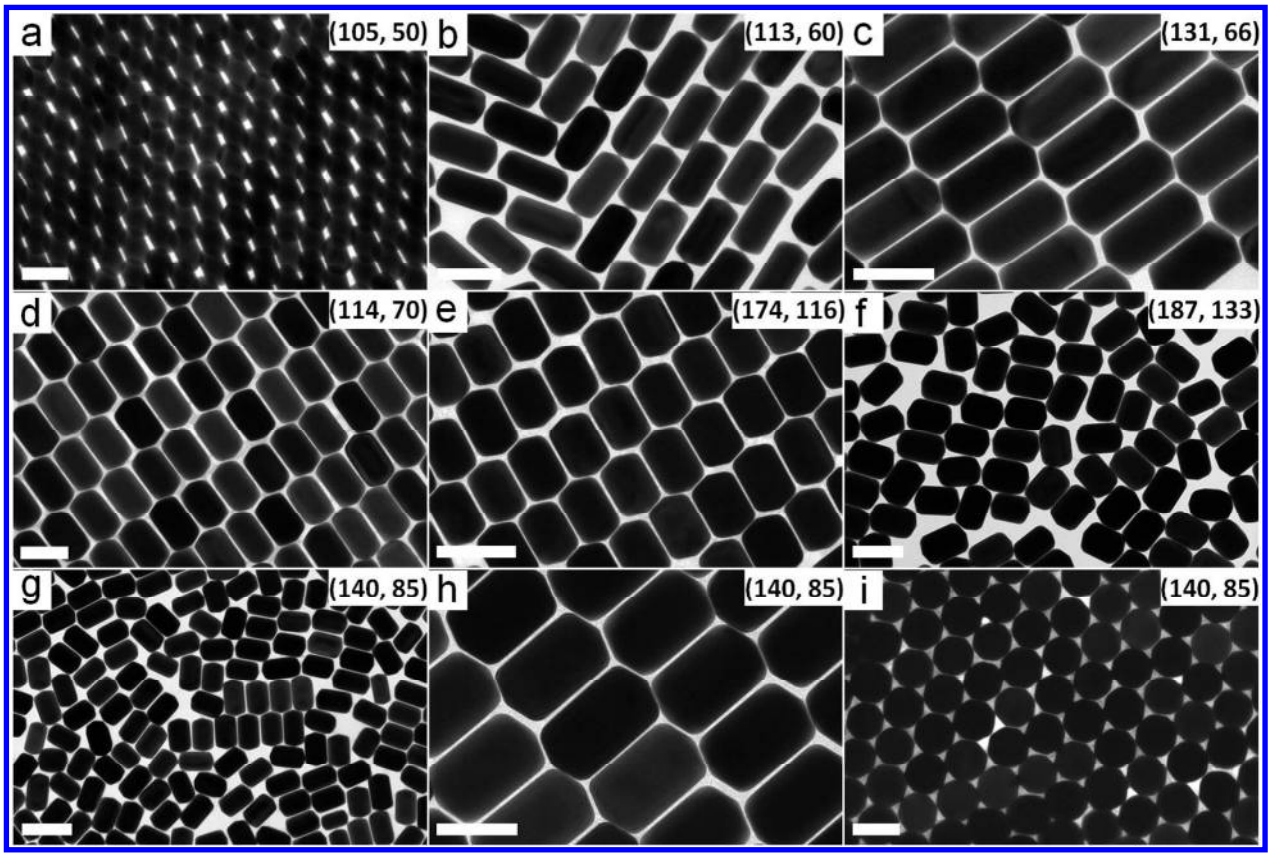


**Figure 6.** (a-i) TEM images of gold NRs having LSPR wavelengths shorter than 700 nm and diameters greater than 50 nm. Insets are the average length and diameter (in nm) of the NRs determined by measuring the dimensions of at least 50 NRs from their TEM images. The growth conditions are detailed in Table S5. Scale bars: a-d) 100 nm, e-g) 200 nm, h-i) 100 nm.

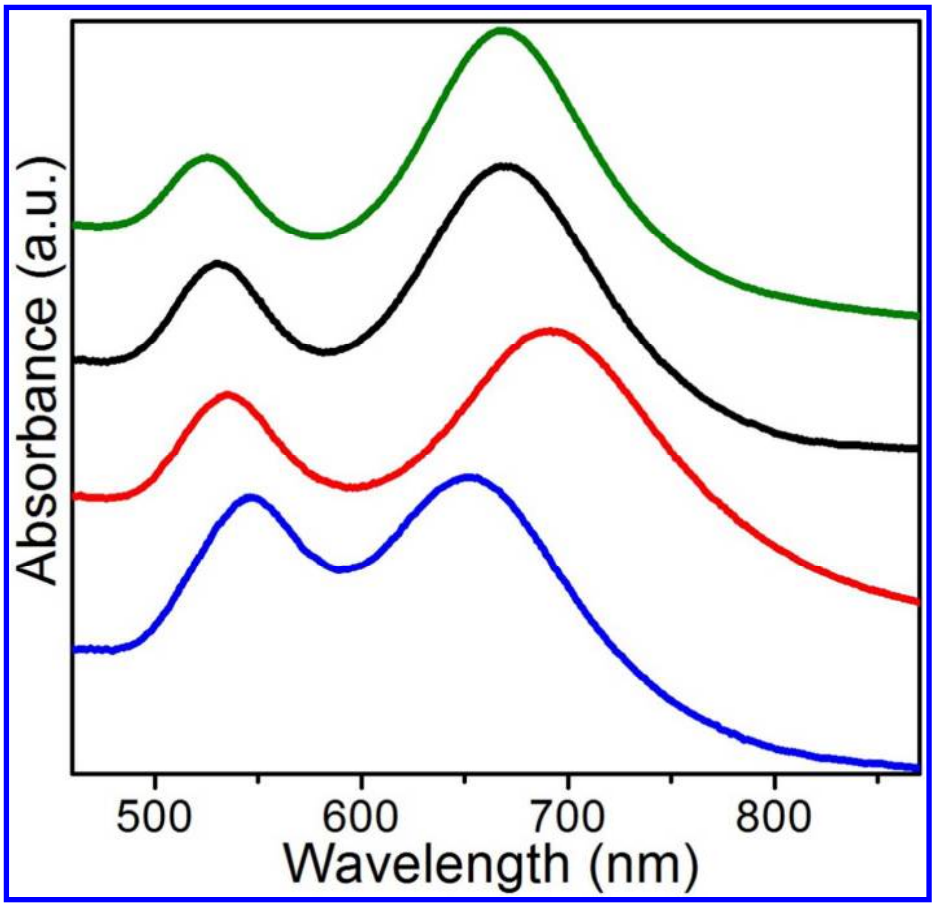


**Figure 7.** Normalized extinction spectra of gold NRs shown in Figures 6a (green curve), 6b (black curve), 6c (red curve) and 6d (blue curve). The spectra have been offset vertically for clarity.

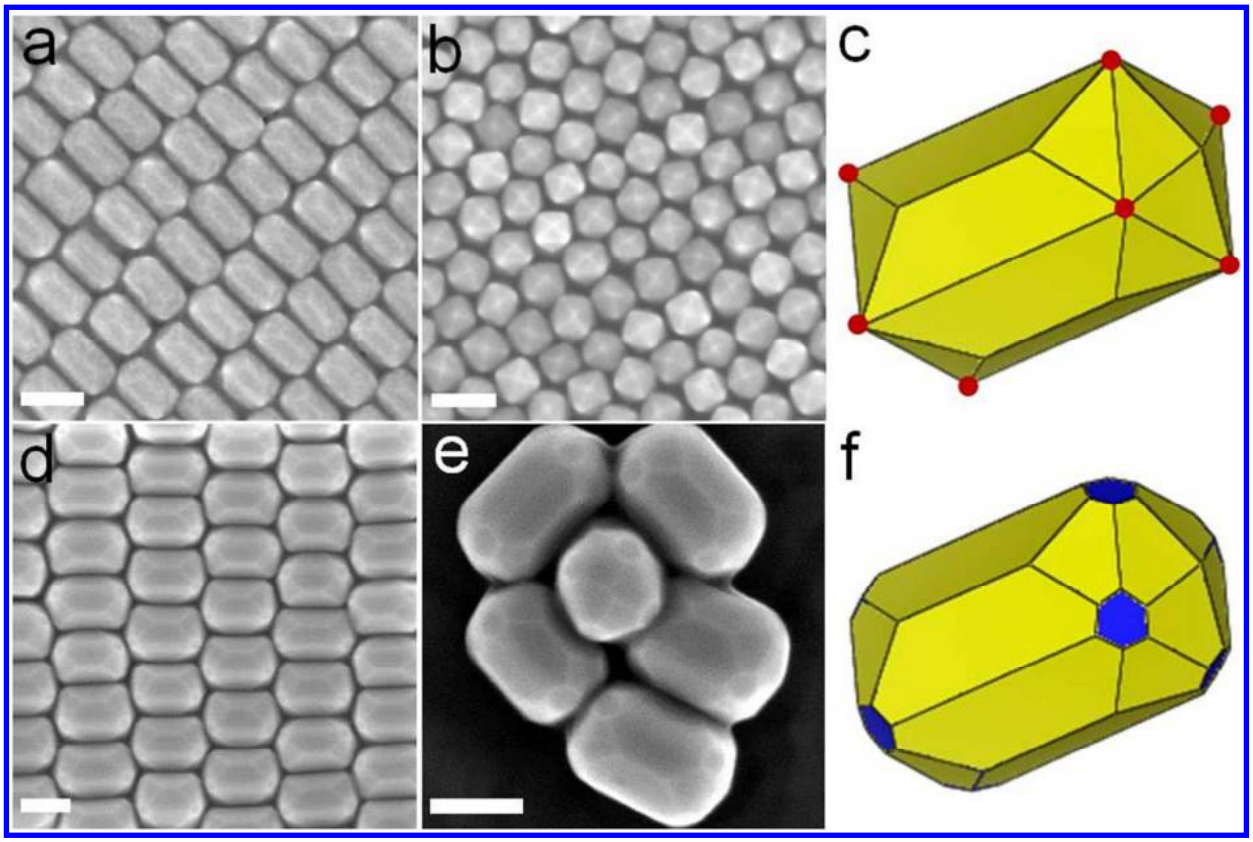


**Figure 8.** SEM images of (a) horizontally and (b) vertically aligned gold NRs (the same sample shown in Figure 6d) having dimensions of (114.2±5.1) nm x (69.8±3.1) nm and (c) structural model of ETHH NRs. Red dots: vertices where six facets meet. (d-e) SEM images of gold NRs (the same sample shown in Figure 6e) having diamensions of (173.7±9.1) nm x (115.6±4.0) nm and (f) structural model of truncated ETHH NRs. All scale bars represent 100 nm.

Table of Contents (TOC) Graphic